Implementation of an elasto-viscoplastic constitutive law in Abaqus/Standard for an improved characterization of rock materials

Implementation of an elasto-viscoplastic constitutive law in Abaqus/Standard for an improved characterization of rock materials

Nguyen S.K.[1], Volonté G.[2], Musso G[1]., Brignoli M.[2], Gemelli F.[2] and Mantica S.[2]

[1]Politecnico di Torino, [2]Eni S.p.A.

***Abstract**: Subsidence modeling is an important activity in the oil and gas industry, for the environmental and operational implications associated to this phenomenon. Abaqus/Standard has been used for many years in Eni as the main numerical simulator for studying the geomechanical behavior of reservoirs. The results of a large campaign of acquisition of subsidence monitoring data in conjunction with the advanced analysis of laboratory experiments have shown that, in some cases, an improved mechanical characterization can be tailored to better capture the complex behavior of the reservoir rock under the effect of underground fluid withdrawal. In this work we first present an implementation in Abaqus/Standard of an elasto-viscoplastic model – namely the Vermeer and Neher model – as user defined material by means of the UMAT subroutine. Next, we provide the results of various simulations of laboratory tests that were performed to investigate its capability to identify the main features of the behavior of reservoir sands, also including time dependency. Finally, we show a preliminary application to a synthetic, nonetheless realistic, reservoir model that has been performed to assess the capabilities of the elasto-viscoplastic model in the simulation of subsidence evolution.*

***Keywords**: Geomechanics, Subsidence, Constitutive models, Abaqus/Standard, UMAT, Oil&Gas*

1. Introduction

Geomechanics plays an important role during the exploitation of a hydrocarbon reservoir. The stress changes and the strain of the rocks caused by the withdrawal of fluids from the subsurface have to be accurately evaluated in order to properly design wells, platforms and all the other field facilities. Particularly, oil companies spend great efforts in the study of the subsidence phenomenon to provide the authorities with reliable evaluations of the environmental impact of their activities and to plan the eventually required mitigation strategies.

Finite element models are generally considered to be the most effective tools for subsidence simulation and forecast. In the last 15 years Eni has routinely used Abaqus as the standard simulation software [Monaco *et al.*, 2011] for studies at both well scale (wellbore stability and sand production) [Topini *et al.*, 2008; Volonté *et al.*, 2013] and reservoir scale (subsidence) [Capasso and Mantica, 2006].

One of the main advantages of using numerical models for geomechanical simulations is the possibility to describe the mechanical behavior of the geomaterials by means of complex and

suitable constitutive laws. The modeling methodology currently and successfully employed by Eni for the analysis of subsidence phenomena [Gemelli *et al*., 2015] is based on the 1-way coupled approach to hydro-mechanical behavior [Gambolati *et al*., 2005] and on the elasto-plastic Modified Cam Clay model [Roscoe and Burland, 1968] as constitutive law for the stress-path dependent response of the subsurface sediments.

Laboratory tests performed on certain reservoir rocks have evidenced a complex mechanical behavior of the cored materials (such as creep, relaxation, strain rate dependency and aging) that indicates a time and load rate dependence of the measured deformations. In addition, surface displacement monitoring data that became available in the last years suggested that reproducing these features by means of elasto-viscoplastic constitutive laws can further improve the capability of the numerical models to simulate the temporal evolution of the observed subsidence.

The elasto-viscoplastic model of Vermeer and Neher [Vermeer and Neher, 1999] is particularly attractive due to the limited number of parameters needed for its definition. Moreover, each parameter has a clear physical meaning and standard laboratory experiments are sufficient for its determination.

In this work it is first presented the implementation of the Vermeer and Neher model in Abaqus/Standard by means of the user subroutine UMAT. Next, the validation of our approach through the comparison of numerical simulations versus laboratory test measurements is shown. Finally, a realistic reservoir scale application is presented.

2. Vermeer-Neher constitutive model

We model the behavior of reservoir materials under complex loadings with the constitutive model proposed by Vermeer and Neher. This model is built on the concept of isotache [Šuklje, 1957] associated with a visco-plastic modeling approach modified from the overstress theory [Perzyna, 1964]. According to the isotache concept, the stress-strain relationship depends on the strain rate. Notably, the stress strain curves of a given material that is isotropically compressed at different strain rates will be parallel lines: the lower strain rates leading to greater volume strains. According to the modified overstress theory, plastic and viscous strains can be merged together since they both represent non-recoverable strains: visco-plastic strains are then evaluated with respect to a plastic potential function, which refers to a reference strain rate. To summarize, the mechanical behavior of the material is decomposed into elastic and visco-plastic mechanisms as shown by the following equation:

$$\dot{\boldsymbol{\varepsilon}} = \mathbf{D}^{-1}\,\dot{\boldsymbol{\sigma}}' + \frac{1}{\alpha}\cdot\frac{\mu^*}{\tau}\left(\frac{p^{eq}}{p_p^{eq}}\right)^{\frac{\lambda^*-\kappa^*}{\mu^*}}\cdot\frac{\partial p^{eq}}{\partial \boldsymbol{\sigma}'} \tag{1}$$

with:

$$p^{eq} = p' + \frac{q^2}{M^2 p'} \tag{2}$$

$$p' = \frac{1}{3}\left(\sigma'_1 + \sigma'_2 + \sigma'_3\right) \tag{3}$$

$$q = \frac{1}{\sqrt{2}}\sqrt{(\sigma'_1 - \sigma'_2)^2 + (\sigma'_2 - \sigma'_3)^2 + (\sigma'_3 - \sigma'_1)^2} \tag{4}$$

$$\alpha = \frac{\partial p^{eq}}{\partial p'} \tag{5}$$

$$p_p^{eq} = p_{p0}^{eq} . \exp\left(\frac{\varepsilon_v^c}{\lambda^* - \kappa^*}\right) \tag{6}$$

where p_p^{eq} is a generalized pre-consolidation pressure (Figure 1) and p_{p0}^{eq} its initial value (Figure 2), *p'* is the mean effective pressure, *q* is the deviatoric stress, ε_v^c is the cumulative visco-plastic volumetric strain, τ is a reference time usually set equal to 24 hours, ***D*** is the elastic stiffness tensor and κ^*, λ^*, μ^* are 3 material parameters.

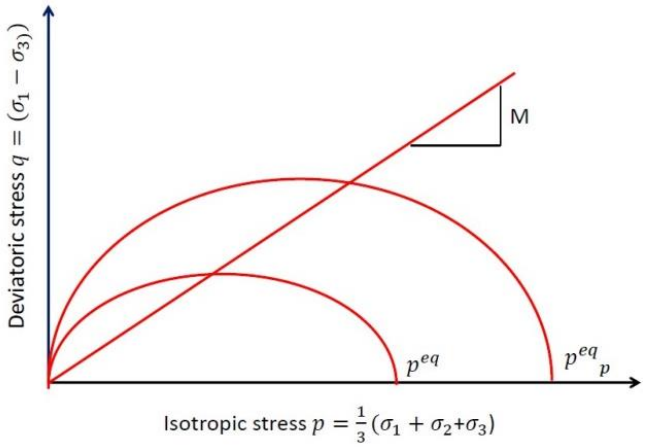

Figure 1. Diagram of p^{eq} ellipse in a p-q plane.

The components of the elastic stiffness tensor are fully defined through the Poisson's ratio ν and the Young's modulus *E*. It is worth noting that the Young's modulus is not constant but it depends on the mean effective pressure as it follows:

$$E = \frac{3(1-2\nu)}{k} p' \tag{7}$$

The main advantage offered by the constitutive model herein adopted consists in the clear physical meaning of all its parameters, which can be obtained directly from laboratory tests (e.g. isotropic compression tests performed at constant strain rate and creep tests).

Typical results of such tests on reservoir materials are shown in Figure 2, which clarifies the physical meaning of the model parameters too. The swelling index κ^* is identified as the slope of volumetric strain vs. axial stress in natural logarithmic scale where the behavior of material is elastic. The compression index λ^* is the slope in the same graph where the behavior is elasto-plastic. These two parameters must be determined at constant strain rate condition. The initial pre-consolidation stress p_{p0}^{eq} is identified at the point where the mechanical behavior switches from elastic to visco-plastic.

In order to identify the parameter μ^*, it is required to perform an isotropic compression test at constant strain rate until the mean stress p' becomes higher than the original pre-consolidation stress p_{p0}^{eq}. Then the stress is kept constant for a sufficient time: in virtue of the viscous behavior, strains will continue anyway to increase. The creep index μ^* is then given by the slope of the volumetric strain-time curve in natural logarithmic scale. Figure 2 provides an example of the identification of this parameter.

The parameter M represents the slope of the critical state line in the (p',q) space, and can be obtained through triaxial compression tests. For reservoir materials it is usually in the range between 1.2 and 2.0.

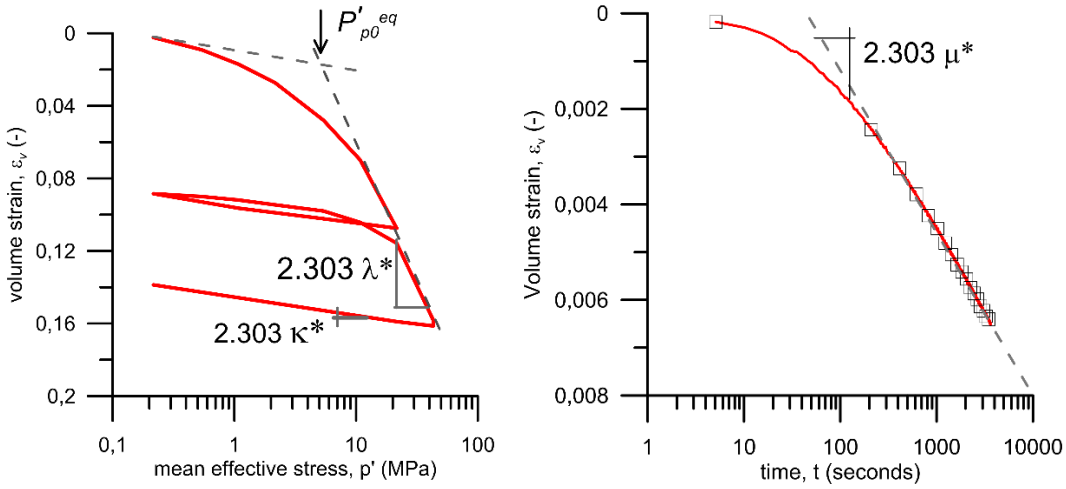

Figure 2. Identification of κ^*, λ^* and pre-consolidation pressure from an isotropic compression test (left) and μ^* from a creep test.

2.1 Implementation in Abaqus

The implementation in Abaqus of the user subroutine for the Vermeer-Neher model, requires the definition of the Jacobian matrix $\boldsymbol{J}$ of the constitutive model. By means of Equation 1, it is possible to deduce:

$$\dot{\boldsymbol{\sigma}} = \boldsymbol{J}.\dot{\boldsymbol{\varepsilon}}^{tot} - \boldsymbol{J}.\dot{\boldsymbol{\varepsilon}}^{visp} = \boldsymbol{J}.\dot{\boldsymbol{\varepsilon}}^{tot} - \boldsymbol{J}.\frac{1}{\alpha}.\frac{\mu^*}{\tau}\left(\frac{p^{eq}}{p_p^{eq}}\right)^{\frac{\lambda^*-\kappa^*}{\mu^*}}.\frac{\partial p^{eq}}{\partial \boldsymbol{\sigma}'} \tag{8}$$

where:

$$\boldsymbol{J} = \begin{bmatrix} J1 & J2 & J2 & 0 & 0 & 0 \\ J2 & J1 & J2 & 0 & 0 & 0 \\ J2 & J2 & J1 & 0 & 0 & 0 \\ 0 & 0 & 0 & J3 & 0 & 0 \\ 0 & 0 & 0 & 0 & J3 & 0 \\ 0 & 0 & 0 & 0 & 0 & J3 \end{bmatrix} \quad \textit{with} \quad \begin{aligned} J1 &= \frac{E(1-\nu)}{(1+\nu)(1-2\nu)} \\ J2 &= \frac{E\nu}{(1-2\nu)(1+\nu)} \\ J3 &= \frac{E}{(1+\nu)} \end{aligned} \tag{9}$$

In an Abaqus UMAT subroutine, the calculated values of variables must be stored in a state-dependent solution array so that they can be used in the subsequent increment. In this subroutine, there are 11 variables which must be stored in state-dependent array STATEV: α, the variable $tp = \frac{1}{\alpha}.\frac{\mu^*}{\tau}\left(\frac{p^{eq}}{p_p^{eq}}\right)^{\frac{\lambda^*-\kappa^*}{\mu^*}}$, the 6 components of $\frac{\partial p^{eq}}{\partial \boldsymbol{\sigma}}$, the cumulative volumetric strain of visco-plastic mechanism ε_v^c and the consolidation pressure (Equation 6).

In Abaqus/CAE dialogue box or in the keyword *`USER MATERIAL`, the 6 model parameters have to be defined in the following order: κ^*, λ^*,μ^*, M, ν, p_{p0}^{eq}.

3. Validation of the implementation

In this section, the Vermeer-Neher model and its implementation as Abaqus/Standard user subroutine are compared against experimental test results by performing two single-element simulations. In the first one, an oedometric (i.e. uniaxial strain) test performed on a sample of reservoir rock is simulated by means of the Vermeer-Neher model. In the second one, both the Vermeer-Neher model and the elasto-plastic Modified Cam Clay model are adopted for the simulation of a stress path obtained by considering the pressure changes expected in a real field.
Both the simulations are performed on a single cubic element by assuming oedometric strain boundary conditions: the displacements of the four vertical faces are constrained only in the horizontal direction, while the ones of lower one are constrained in all directions.

3.1 Oedometric test

In the typical oedometric test, the load is incrementally increased/decreased by varying instantaneously the load applied in the top surface of the sample every 24 hours. In this case, a creep phase, in which the load is kept constant for 15 days, has also been added.

The initial height is 20 mm, thus the time required for primary consolidation is relatively short: in this case, it was assumed that the complete consolidation is reached in about 1 hour, so that the remaining 23 hours of each step can be considered as creep phases.

In this test, the initial stress state is isotropic, with axial and radial stresses equal to 0.1 MPa, then the vertical load is increased or decreased by following the sequence described in Figure 3 that includes also the 15 days creep phase at a constant axial stress of 30 MPa.

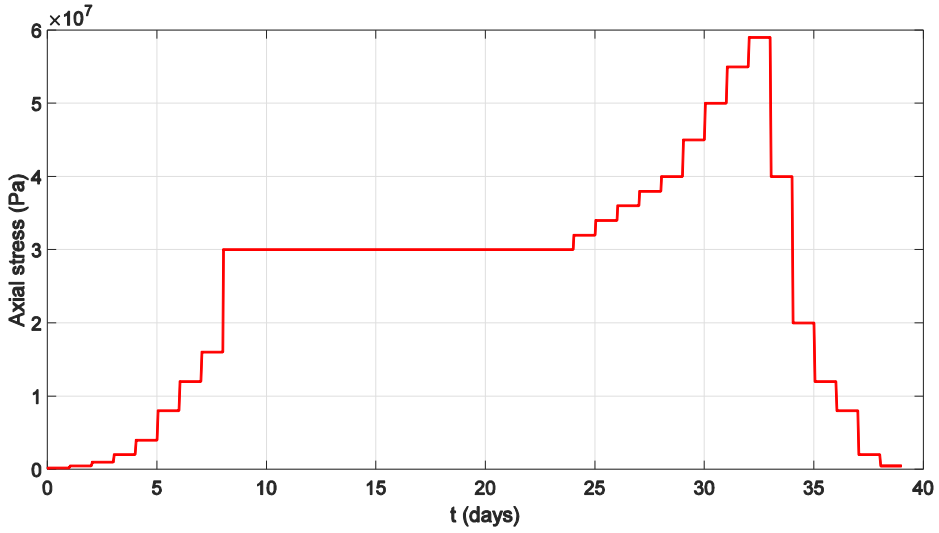

Figure 3. Loading paths of the oedometric test.

By applying procedures, similar to the ones described in section 2, to the experimental data, it has been possible to identify the parameters of the Vermeer-Neher model for the rock at hand. A sensitivity analysis has been performed by adopting 3 different values of swelling index κ^*. The adopted parameters are shown in Table 1.

Parameter	λ^*	κ^*	μ^*	M	p_{p0}^{eq}
Value	0.0521	0.0053/0.008/0.01	0.0004/0.0011/0.0033	1.46	2.85 MPa

Table 1. Parameters of the modeling for oedometric test.

Figure 4 shows the comparison between the results of the simulations and the experimental data. It is possible to highlight that the model is able to reproduce correctly the behavior of the material during loading and creep phases. Predictions during unloading are also good, although they might be improved adopting a rotational hardening scheme [Leoni et al., 2008]: this was not implemented here to keep this model as simple as possible.

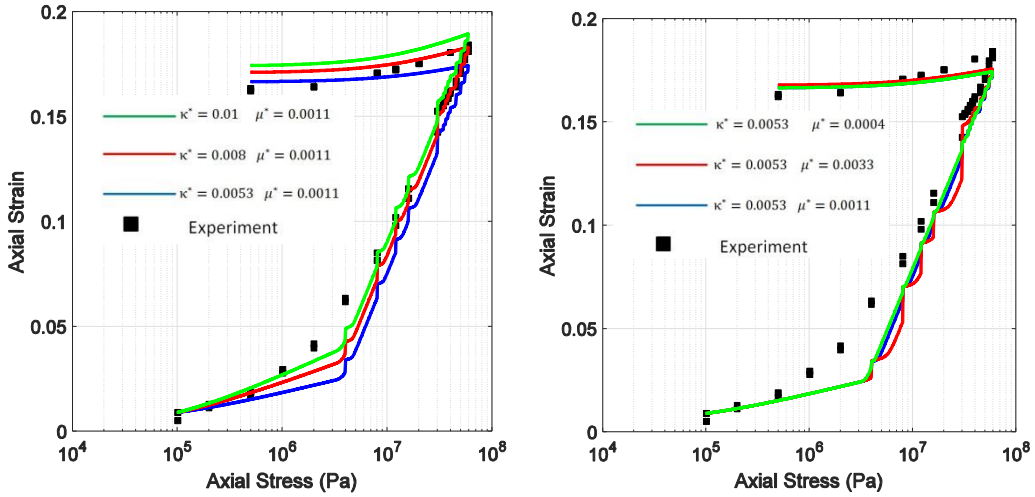

Figure 4. Modeling results of oedometric test with different values of κ* (left) and μ* (right).

3.2 Stress path from a real reservoir

To test the behavior of the Vermeer-Neher model under stress paths similar to the ones that are expected in a hydrocarbon reservoir, the pore pressure history in a point at depth of 906 m has been extracted from a real reservoir case flow-dynamic simulation. Such pore pressure history has been imposed to a single element subjected to uniaxial strain boundary conditions and to a vertical load of 16.8 MPa (corresponding to the weight of the overlying sediments). The resulting stress path is shown in Figure 5 and the adopted parameters for the Vermeer-Neher model are listed in Table 2.

With the aim of comparing the response of the elasto-viscoplastic model at hand with that one provided by the Modified Cam Clay Model, a further simulation of realistic reservoir conditions has been performed by using both the constitutive models.

The parameters λ and κ of the Modified Cam Clay model are related to the parameters of the Vermeer-Neher model as it follows:

$$\lambda = \lambda^{*}(1+e) \tag{1}$$

$$\kappa = \kappa^{*}(1+e) \tag{2}$$

where e is the void ratio, which in both simulations has been assumed equal to 0.3, therefore the parameters λ and κ of the Modified Cam Clay model are equal, respectively, to 0.11258 and 0.0375.

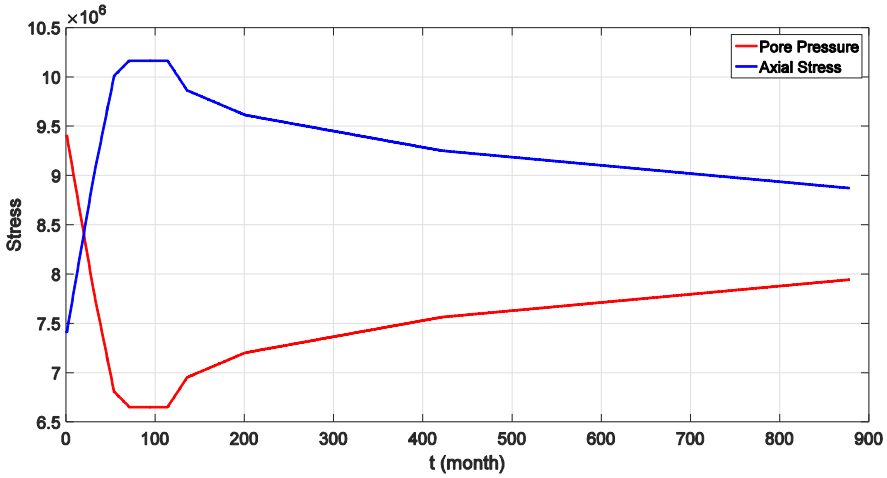

Figure 5. Evolution of pore pressure and axial stress (measured in Pa).

Parameter	Value
κ^*	0.02887
λ^*	0.0866
μ^*	0.001
M	1.5
ν	0.3
p_{p0}^{eq}	7 MPa

Table 2. Parameters for the simulation of the real case.

It has been assumed an initial vertical stress of 7.4 MPa and an initial horizontal one of 5.6 MPa coherently with the depth and the initial pore pressure of the simulated point of the reservoir. The initial state is normally consolidated in both simulations.

The results of the simulations are shown in Figure 6 and Figure 7. It is possible to observe that the responses of the two models are similar during the initial loading phase, i.e. while the pore pressure is continuously decreasing. On the contrary, when the pore pressure decreases so slowly to get constant for some months, the Vermeer-Neher model, as opposed to the Modified Cam Clay model, is able to describe the softer behavior of the material due to the reduced loading rate and the axial strain at almost constant effective stress. Finally, during the unloading due to pore pressure increase, the behavior of material is mainly elastic and is governed by swelling index in both simulations.

These results highlight the similarities between Modified Cam Clay and Vermeer-Neher models when loading rates are almost constant. The elasto-viscoplastic description given by the latter, however, allows reproducing specific features of the behavior of the material, such as creep and strain rate dependency, by adding only one parameters to the ones already existing in the Modified Cam Clay.

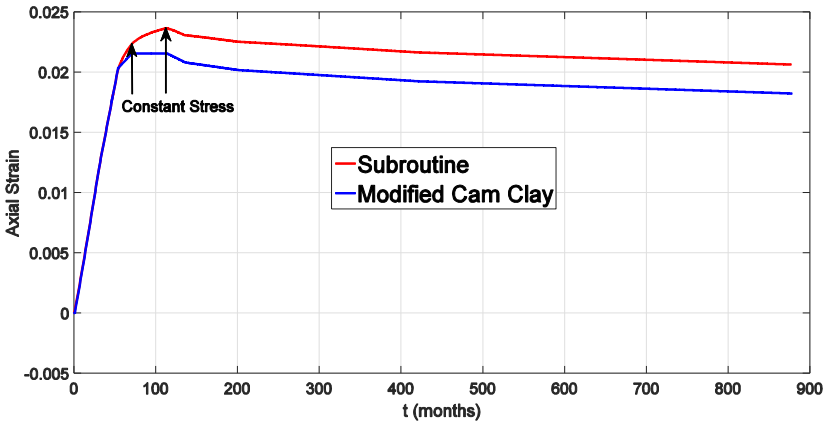

Figure 6. Evolution of axial strain with time.

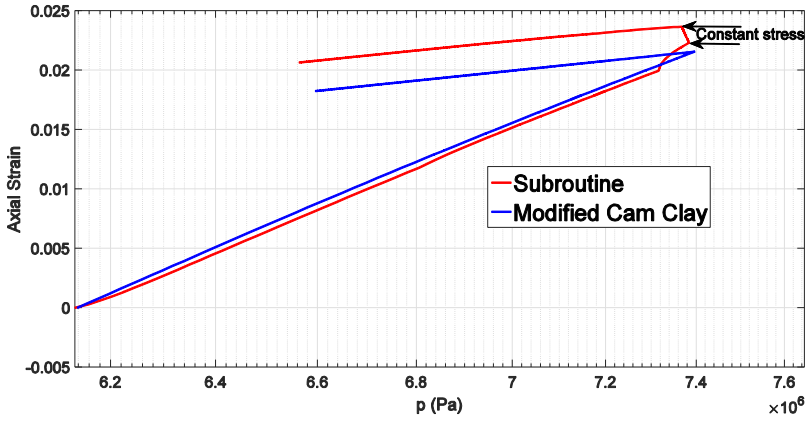

Figure 7. Evolution of axial strain with mean effective stress.

4. Reservoir scale application

In this section, a realistic field application of the Vermeer-Neher constitutive law is shown. This law has been adopted in the geomechanical model of a synthetic reservoir with the aim of simulating the subsidence above the field itself.

The considered synthetic reservoir is saturated with oil, gas and water and its average depth is about 2350 m. The initial average porosity of the mineralized region is 0.2.

The production is assumed to start on 1st January 1967 and to continue until 1983. During this phase, the maximum oil production rate is 3000 Smc per day. The wells were closed from 1983 to 2003 and, then, the production restarts and continues for further 10 years. The production and the evolution of pore pressures in the reservoir are simulated by means of a numerical flow-dynamic simulator. The resulting oil production profile and the evolution of the average reservoir pore pressure are shown in Figure 8.

To correctly evaluate the evolution of the stress state above and around the reservoir and, consequently, correctly predict the evolution of land subsidence, the geomechanical model has to include also the description of the rocks surrounding the reservoir. Figure 9 shows how the geometry of the flow-dynamic model has been extended in the geomechanical one to include overburden, underburden and sideburden regions.

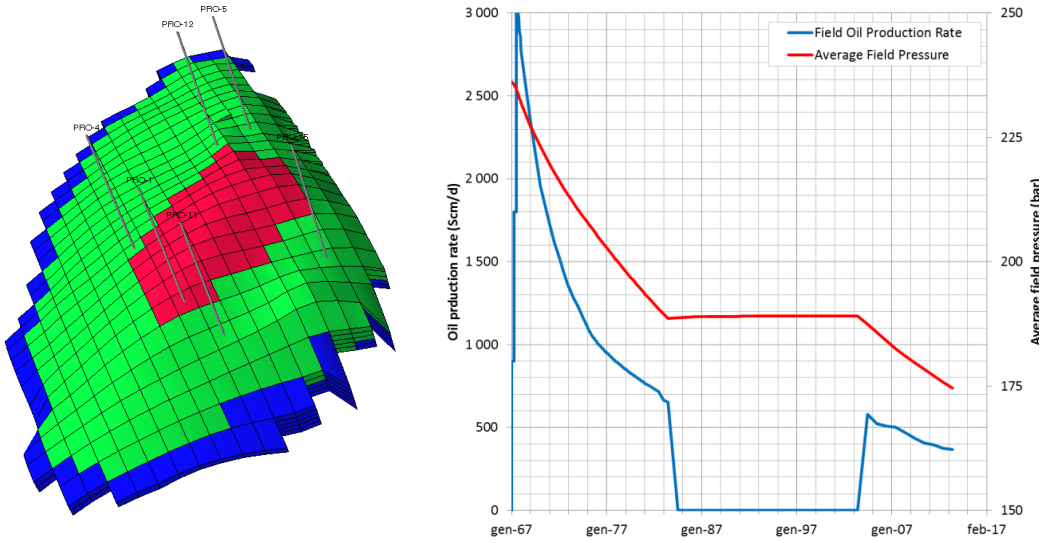

Figure 8. Geometry of the reservoir (left picture, where green is for oil, red for gas and blue for water) and evolution of field production and pressure (right).

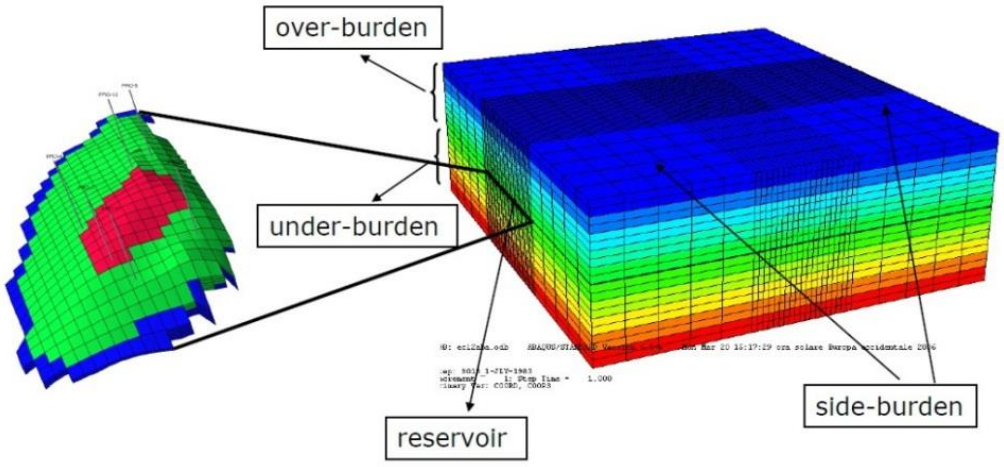

Figure 9. Geometry of the geomechanical model.

The initial void ratio of the model is identified from the initial porosity ϕ of reservoir by means of the following equation:

$$e_{ini} = \frac{\phi}{1-\phi} \tag{3}$$

The initial stress state is identified by determining, first, the total vertical stress by integrating the bulk density on depth and, then, the horizontal one is determined proportionally to the vertical one as shown in Figure 10.

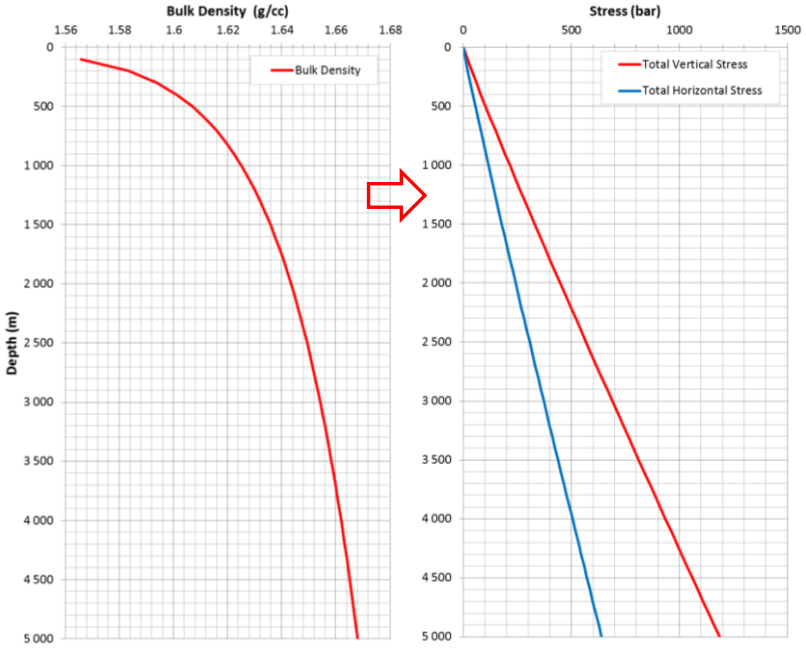

Figure 10. Bulk density and initial stresses profiles.

The boundary conditions of the model constrain the horizontal displacements of the lateral faces and fully blocks the bottom face.

The load applied to the model is the gravity force while the pore pressure fields, computed in the flow dynamic simulation, are imposed to the Abaqus model nodes as internal boundary conditions at each time increment.

The reservoir rocks are described by means of the Vermeer-Neher constitutive law and the assumed values of its parameters are shown in Table 3.

κ^*	λ^*	μ^*	M	ν	p_{p0}^{eq}
0.0287	0.086	0.001	1.33	0.3	$1.2p_{ini}^{eq}$

Table 3. Parameters of the Vermeer-Neher model.

The constitutive behavior of the rocks surrounding the reservoir is described by a linear elastic law, with Poisson's ratio equal to 0.3 and Young's modulus depending on depth.
A simulation has also been performed by adopting the Modified Cam Clay model in order to highlight the differences in the subsidence evolution obtained by means of the traditional elasto-plastic approach and the elasto-viscoplastic one. The swelling and compression index of the Modified Cam Clay model used in the simulation were derived from the ones of the Vermeer-Neher model by means of Equations 10 and 11.
Results of a geomechanical subsidence model are usually interpreted in terms of maps of subsidence and the evolution in time of the subsidence at the node of the surface where the maximum value is reached.
Figure 11 shows the subsidence map (in cm) obtained at the end of the simulation by adopting the two constitutive models.

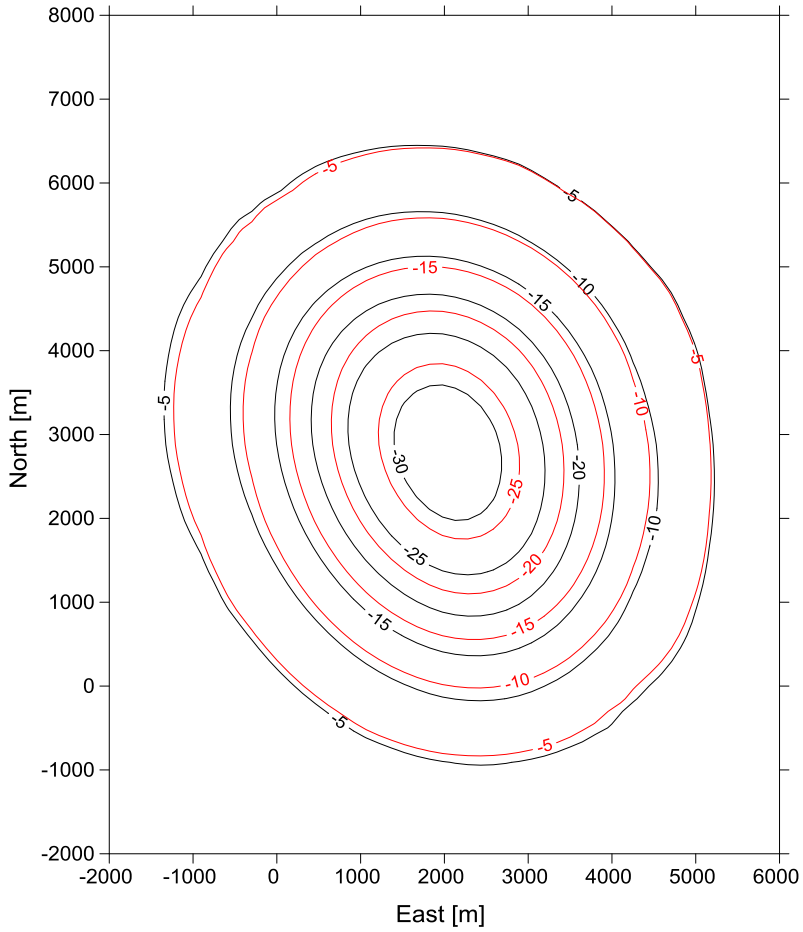

Figure 11. Subsidence map (cm) at the end of the simulation (red lines indicate the Vermeer-Neher model, black lines the Modified Cam Clay).

These maps shows that the differences between the results of the two approaches at the end of the simulations, in terms of extent of the subsidence bowl, are negligible.
The differences in terms of temporal evolution of the subsidence on a node of the surface are more evident, particularly when production is stopped and when it is resumed. In Figure 12 this temporal evolution is shown for the node where the maximum value is reached, which is coincident in the two simulations.
It should be highlighted, first, that the response provided by the Vermeer–Neher model simulates an increase of subsidence while the production is stopped (from 1983 to 2003). On the other hand, during this phase, the response of the Modified Cam Clay model, that does not include any dependence on time or loading rate, does not show any subsidence because the effective stress state is almost constant.

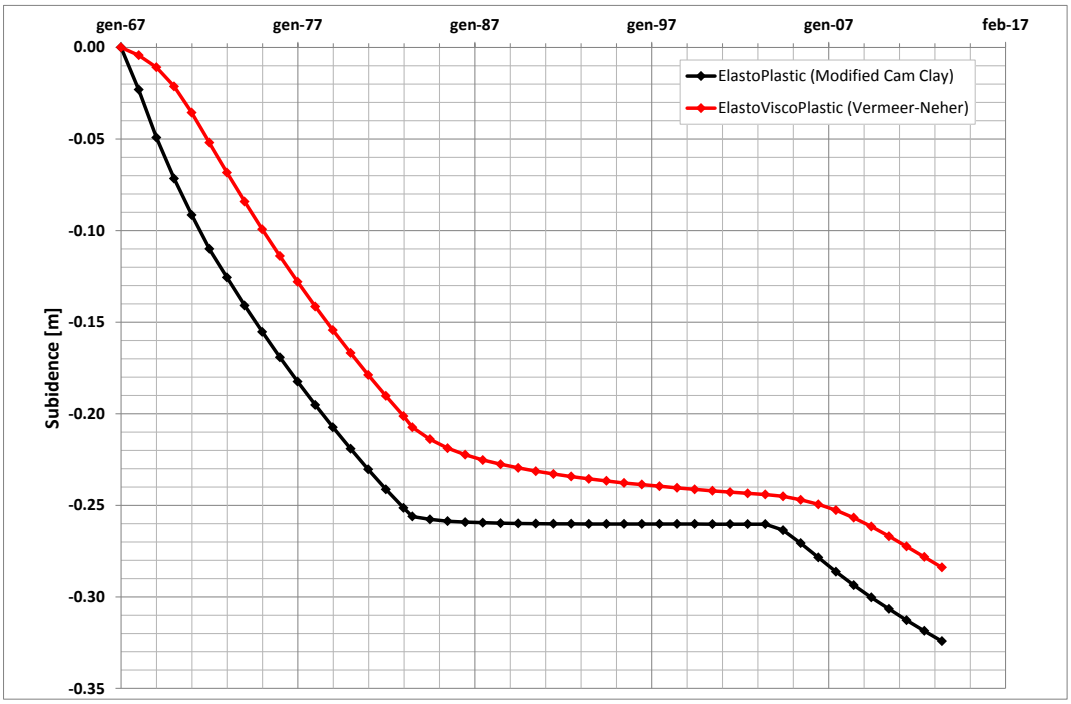

Figure 12. Subsidence simulated with Vermeer-Neher and Modified Cam Clay in the node where the maximum value occurs.

It is possible to observe that in 2003, when the production is resumed, the Vermeer-Neher model provides a stiffer response of the system (Figure 13). This result, which corresponds to the "aging" behavior observed at laboratory scale, can be explained by the increase of both pre-consolidation pressure associated to the volumetric strain of the creep phase as described by Equation 6.

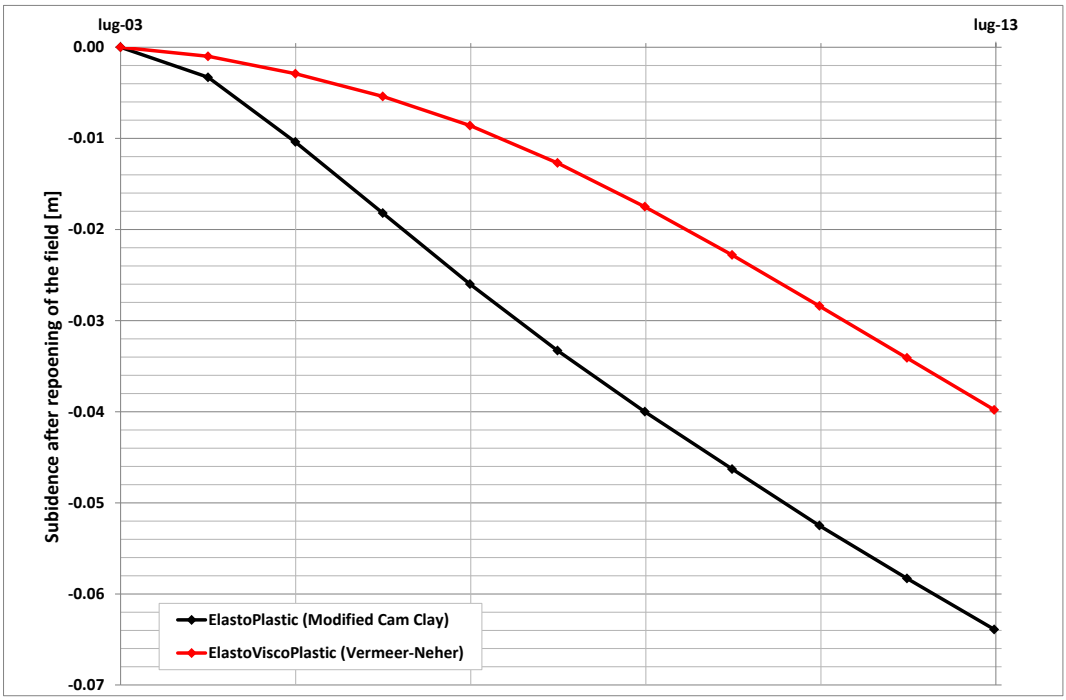

Figure 13. Subsidence simulated with Vermeer-Neher and Modified Cam Clay in the node where the maximum value occurs when the production is resumed.

5. Conclusions

This paper shows the implementation of the Vermeer–Neher elasto-viscoplastic model in Abaqus/Standard by means of the user subroutine UMAT and its validation by means of simulations at laboratory and field scale. The comparison with the laboratory oedometric tests have shown a good accordance between measured data and simulation results. On the other hand, the comparison between the implemented model and the Modified Cam Clay (performed by simulating real stress paths on a single element model) shows the capability of the elasto-viscoplastic model to describe features of the geomaterial behavior, which are not fully captured by classic elasto-plastic models. This capability has been further emphasized by the application of Vermeer-Neher model to a synthetic but realistic field case of subsidence simulation. This application has shown that, unlike the Modified Cam Clay, the elasto-viscoplastic model simulates trends of subsidence that can be correlated to creep and to aging when production is stopped or resumed.

6. References

1. Capasso, G. and Mantica, S. (2006), "Numerical simulation of compaction and subsidence using ABAQUS", Proc. ABAQUS Users' Conference, Boston, USA.
2. Gambolati G., Teatini P., Ferronato M. (2005), "Basic conceptual guidelines for a sustainable gas/oil field development", Proc. 7th Int. Symp. on Land Subsidence, China, 2: 919-924.
3. Gemelli, F., Monaco, S. and Mantica, S. (2015), "Modelling Methodology for the Analysis of Subsidence Induced by Exploitation of Gas Fields", Second EAGE Workshop on Geomechanics and Energy.
4. Leoni, M., Karstunen M. and Vermeer P.A. (2008), "Anisotropic creep model for soft soils", Géotechnique 58, 3, 215-226.
5. Monaco, S., Capasso, G., Datye, D., Vitali, R. (2011), Proc. Simulia Customer Conference, Barcelona, Spain.
6. Šuklje L. (1957), "The analysis of the consolidation process by the isotache method", Proc. 4th Int. Conf. on Soil Mech. and Found. Engng., London, Vol. 1, Butterworths, London, pp. 200–206.
7. Perzyna P. (1964), "The constitutive equations for rate sensitive plastic materials", Quart. Appl. Mech., 20, 321-332.
8. Roscoe K. H. and Burland J. B. (1968), "On the generalized stress-strain behaviour of 'wet' clay", Engineering Plasticity, Cambridge Univ. Press, 535-609.
9. Topini, C., Bertolo, F. and Mantica, S. (2011), "Buckling analysis for the long-term integrity evaluation of a hydrocarbon well", Proc. Simulia Customer Conference, Barcelona, Spain.
10. Vermeer, P.A., and Neher, H.P (1999), "A soft soil model that accounts for creep", Proc. Int. Synp. "Beyond 2000 in Computational Geotechnics", Amsterdam, pp. 249-261, Balkema, Rotterdam.
11. Volonté, G., Scarfato, F., Brignoli, M. (2013), "Sand prediction: a practical finite-element 3D approach for real field applications", SPE Productions & Operations, SPE 134464.

7. Acknowledgments

The authors acknowledge Eni S.p.A. for the permission to publish this paper.